Chapter 4

Single-channel sEMG based control of multi-functional prosthetic hand

4.1 Introduction

There is rapid development in the field of upper-limb prosthesis due to the advancement in the EMG sensor, actuator, controller, and design-fabrication technologies. Various available prosthetic hands with multi-degrees of freedom (DOF) can provide decent grasping capability and a sufficient number of grip patterns to users (Endo et al. 2011; Belter et al. 2013). Although these hands offer several features and functionalities, their cost is excessively high; also, these require a significant number of training sessions for their accurate performance (Cordella et al. 2016; "I-Limb Quantum"; "Bebionic Hand"; "Michelangelo Prosthetic Hand"; "VINCENTevolution 3").

The complete control of the multi-DOF myoelectric hand requires a large number of EMG sensors that significantly increases the cost and complexity of the system. Acquisition of multi-channel EMG data involves placing multiple bipolar electrodes or high-density electrode arrays on the forearm muscle. Such configuration makes the system bulky, complex, costly and less robust (Cipriani, Controzzi, and Carrozza 2011; Al-Timemy et al. 2013; Geng et al. 2016; Khushaba et al. 2017). The currently available prosthetic devices are controlled through a pattern recognition scheme based on the multiple inputs from EMG sensors and other devices like pressure sensors, accelerometers, mobile phones, etc. Pattern recognition (PR) based control scheme includes two significant steps, i.e., feature extraction and classification, for attaining higher output performance. First, the acquired EMG signals are transformed into a feature vector in the feature extraction process that corresponds to different hand activities. And then, the extracted features are further classified to recognize the specific motion patterns for controlling prosthesis (Englehart et al. 1999; Oskoei and Hu 2008; Ahsan, Ibrahimy, and

Khalifa 2011). The control schemes utilizing only single-channel EMG data to classify multiple hand activities have attained popularity currently.

A simple approach for prosthetic control was proposed by utilizing single-channel EMG to classify four different hand motions (Chan, Lam, and Parker 2000). Vijay Pal et al., 2008 classified low level and complex muscle contraction like finger flexion using a single-channel EMG system for controlling prosthetic devices (Singh and Kumar 2008). Giuseppina Gini et al., 2012 acquired and analyzed EMG signals (for different muscular contractions) by positioning electrodes on the forearm to distinguish multiple hand movements for the application in prosthetics (Gini et al. 2012). Wang et al., 2017 utilized single-channel EMG based PR to generate eight gestures for controlling a prosthetic hand (N. Wang, Lao, and Zhang 2017). A simple and effective technique was presented that utilizes only a single-channel sEMG to recognize up to four gestures for controlling multi-DOF prosthetic hands (Tavakoli, Benussi, and Lourenco 2017). A single-channel sEMG envelope based gesture recognition technique was proposed for robotic application (Wu et al. 2018).

Classification using single-channel EMG has several advantages over multi-channel EMG: (1) it does not require skilled positioning of a large number of electrodes that can make the acquisition setup complex and bulky, (2) lowers overall cost and, (3) reduces the computational complexity and time. Increasing the number of EMG channels will increase the classification accuracy but handling such a large number of featured data sets makes the task complicated (Maitrot et al. 2005; Erim and Lin 2008; S. Arjunan and Kumar 2010; Phinyomark, Phukpattaranont, and Limsakul 2012; S. P. Arjunan, 2008.). The classification of single-channel EMG data remains unpopular for the application of real-time control of multi-functional hand prostheses. The main issues are (1) the single-channel EMG system generates a limited number of patterns, (2) sometimes it becomes hard to distinguish the patterns produced for different activities and, (3) the electrical noise interference associated with the EMG signal. Utilizing EMG envelopes for different contraction levels of forearm muscles rather than using patterns for different hand motions can overcome problems related to single-channel EMG (Wu et al. 2018).

This chapter proposes a multi-functional prosthetic hand that can perform six different grip patterns utilizing a single channel EMG signal from subjects. A previously designed sEMG sensor (in chapter 3) was utilized here for detecting muscular activations in the form of a 0-5 V linear envelope. The EMG signals acquired from the forearm muscles of various subjects for their different levels of muscular contraction were classified using a Fuzzy logic system to enable six predefined hand gestures. The performance parameters such as accuracy, sensitivity, specificity, precision, and F1 score were determined and analyzed to see the effectiveness of classification. Further, the classification based control scheme was implemented in hardware for real-time operation of the developed prosthetic hand. The hand could perform six distinct grip patterns to grasp various objects utilizing EMG signals from subjects.

4.2 Materials and Methods

4.2.1 Electromyography

4.2.1.1 EMG sensor

Surface EMG signals consist of significant information regarding the activation of muscles that can be effortlessly utilized to control prosthetic devices. However, as these signals are influenced by several noises present within and outside the system, their reliable detection becomes complex. Therefore, a dry electrode-based single-channel sensor (described in chapter 3) was employed in this work to record EMG signals from subjects reliably (Prakash, Sharma, and Sharma 2019). The sensor's output is a 0-5 V linear envelope proportional to the strength of muscular contraction. Figure 4.1 displays the basic block diagram of the sensor showing various stages.

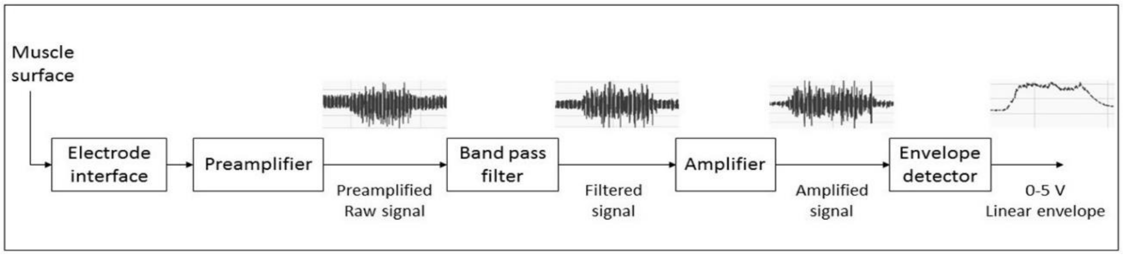

Figure 4.1 Block diagram of the sensor showing different stages.

4.2.1.2 Muscle contractile force

A sensitive band was designed using a force-sensitive resistor (FSR) to measure muscular contractile force in terms of voltage. The FSR sensing area was encased in a 3D printed structure to properly distribute muscular contractile force over the contact surface area (Esposito et al. 2018). Figure 4.2(a) shows the sensing portion of the designed FSR band, and 4.2(b) depicts the voltage divider circuit for translating the change in resistance of FSR to the voltage output. The designed FSR band was attached to the flexor carpi ulnaris muscle on the forearm, as shown in Figure 4.2(c). Using the voltage output from the FSR band, a maximum of six different muscular contractile forces were defined in terms of % of maximum voluntary contraction (MVC) for recording EMG data. Table 4.1 describes the allocation of six different levels of muscle contractions in which the sixth level corresponds to MVC.

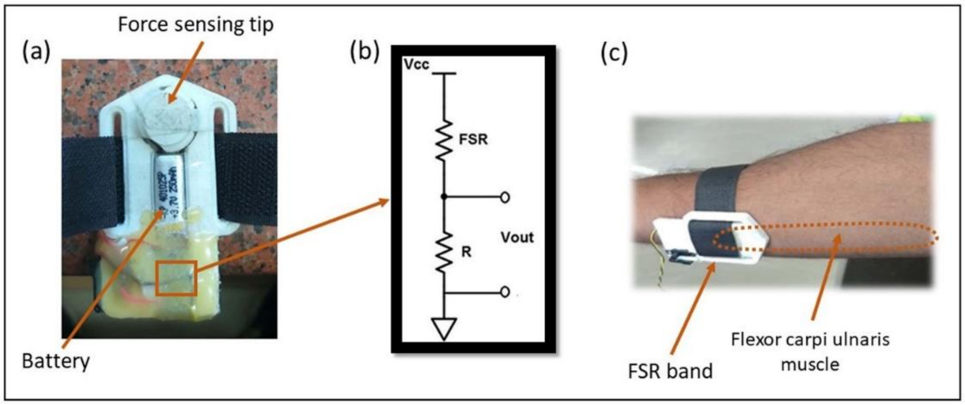

Figure 4.2 (a) FSR band, (b) translating circuit, (c) attachment of FSR band on the forearm.

FSR output voltage (V)	Contraction	Contraction level
0.8	25% of MVC	1
1.25	40% of MVC	2
1.7	55% of MVC	3
2.2	70% of MVC	4
2.8	85% of MVC	5
3.2	MVC	6

Table 4.1. Contraction levels for recording EMG data.

4.2.1.3 Sensor attachment to the forearm

Both the FSR band and the sEMG sensor were placed close to each other on the flexor carpi ulnaris muscle of the forearm, as depicted in Figure 4.3(b). The specified muscle on the forearm is directly responsible for the flexion of fingers and movement of the wrist (Supuk, Skelin, and Cic 2014; Lobo-Prat et al. 2014). FSR band measures the level of muscle contraction (in voltage) in terms of percentage maximum voluntary contraction (%MVC). At the same time, the sensor measures the EMG signals for each contraction level. Since the designed EMG sensor is dry electrode-based, it was attached to the forearm muscles using velcro tape. Figure

4.3(a) shows the attachment of the sEMG sensor to the residual forearm stump of a left-hand amputee.

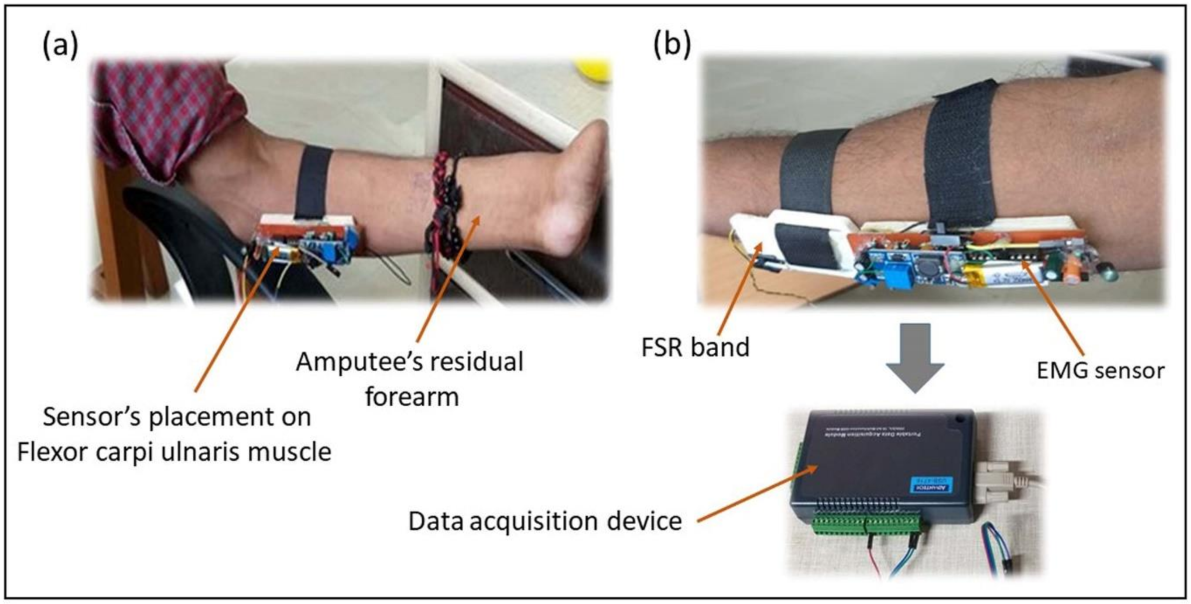

Figure 4.3 (a) Sensor attached on the forearm muscles of a transradial amputee, (b) attachment of sensor and FSR band together on the forearm muscles.

4.2.2 Subjects

EMG signals for fifteen subjects (five amputees and ten intact) were acquired for their different contraction levels (i.e., contractile force) of forearm muscles using the designed sensor. Before conducting this experiment, ethical approval was taken from the ethical committee, institute of medical sciences, BHU, Varanasi, India. Table 4.2 provides the particulars of amputees with their type and reason for amputation, participated in this experiment. In addition, written consent was taken from each subject who participated in this work. The contraction levels were decided based on the force exerted by the flexor muscles on the force-sensitive resistor (FSR) during contraction. As the amputees cannot perform natural hand activities with their residual limb, to maintain consistency in EMG data, similar activities (i.e., contraction of muscles at different forces) were decided for amputees and healthy subjects.

S.no.	Gender	Age	Weight	Type of Amputation	Reason of Amputation
1.	Male	50	85 kg	Transradial (right hand)	Accident
2.	Male	12	25 kg	Transradial (right hand)	Accident
3.	Male	20	50 kg	Transradial (left hand)	Accident
4.	Female	25	52 kg	Transradial (right hand)	By birth
5.	Male	30	61 kg	Transradial (right hand)	Accident

Table 4.2. Details of amputees participated in the experiment.

4.2.3 Experimental protocol and data acquisition

The output of both the devices (i.e., FSR band and EMG sensor) were connected to the analog input ports of the data acquisition (DAQ) device. Data acquisition was executed on the Lab VIEW 2015 software platform at a sampling frequency of 2 kHz. The real-time interface of the DAQ device shows the muscle contraction level and its corresponding envelope of the EMG signal. For EMG recording, all the subjects were instructed to sit comfortably on the chair, with their elbow joint rested on the table. Each subject, watching the computer screen, performed six different levels of muscular contractions as per Table 4.1. For each contraction level, ten repeated EMG data were recorded. Each action (i.e., muscle contraction) was done by the subjects for 5 s and for the same duration, data were recorded. All the contractions done in this study were isometric in which muscle length remains constant (Nazmi et al. 2016).

4.2.4 Feature Extraction

Feature extraction is an important technique for extracting valuable information present in the sEMG signal and eliminating the undesired part and interferences. The feature vector should be carefully selected for the successful classification of the EMG signal. The EMG signal features are chiefly classified as time-domain (TD), frequency domain (FD), and time-frequency domain (TFD). TD features refer to the statistical parameters which are directly derived from the signal amplitude varying with time. On the other hand, FD features give the power spectrum density (PSD) of the signal, which are indirectly computed using various transform techniques. TFD features provide collective information about the time and frequency of the signal. These features can depict frequency-changing details of the signal at distinct time intervals, i.e., non-stationary behavior about the signal (Nazmi et al. 2016).TD features are extensively used for EMG signal classification over FD and TFD features due to their decent performance in low noise environments and lesser computational time as well as complexity (Englehart et al. 1999; Oskoei and Hu 2008; Al-Mulla, Sepulveda, and Colley 2011; Ahsan, Ibrahimy, and Khalifa 2011; Khushaba et al. 2017). Also, the TD features are most suitable for real-time applications like the control of prosthetics. Although the EMG signal is stationary, i.e., its statistical properties change over time, but TD features assume the data as a stationary signal (Phinyomark, Phukpattaranont, and Limsakul 2012). In this work, four TD features were proposed through an extensive literature survey and were computed on LabVIEW using the pre-processed EMG data of 5 s duration. These statistical features in the time domain are described as follows:

(i) Mean Absolute Value (MAV)

The MAV is defined as the average of the absolute value of the EMG signal. It is directly related to the levels of muscular contractions and is applied widely for myoelectric control application.

$$\mathrm{MAV} = \frac{1}{N}\sum_{n=1}^{N}|x_n| \tag{4.1}$$

Where x_n represents the EMG signal in a segment n, and N denotes the length of the EMG signal.

(ii) Integrated EMG (IEMG)

It is the summation of the magnitude of the EMG signal for a given number of samples. It is related to the EMG signal sequence firing point (Phinyomark, Phukpattaranont, and Limsakul 2012).

$$\mathrm{IEMG} = \sum_{n=1}^{N} |x_n| \tag{4.2}$$

(iii) Maximum Value of Signal (MAX)

The maximum value of the EMG signal is its peak amplitude for a given length. This feature is used for a signal whose amplitude swings above zero value.

(iv) Root Mean Square (RMS)

It gives the square root of the average power of the EMG signal calculated for a given period. It is related to the constant force and non-fatigued contraction of the muscle. It is also similar to the standard deviation method.

$$\mathrm{RMS} = \sqrt{\frac{1}{N}\sum_{n=1}^{N} {x_n}^2} \tag{4.3}$$

4.2.5 Classification

The EMG signal features for six different contraction levels of forearm muscles were classified to recognize six predefined gestures of the hand (shown in Figure 4.9) using Fuzzy logic classifier (FLC).

4.2.5.1 Design of classifier

The Fuzzy logic (FL) classifier was designed on LabVIEW utilizing the Fuzzy system designer tool. The Gaussian membership function (MF) was used for the inputs and triangular MF for the output to perform FL classification. The Centre of area (COA) was employed as a method for defuzzification. Based on the knowledge from the different levels of contraction, the rules were formed. The rules created for FLC are mentioned in Table 4.3.

Rules	MAV	IEMG	MAX	RMS	Result
1	Level 1	Level 1	Level 1	Level 1	Fine pinch
2	Level 2	Level 2	Level 2	Level 2	Tripod grip
3	Level 3	Level 3	Level 3	Level 3	Spherical grip
4	Level 4	Level 4	Level 4	Level 4	Fingers flexion
5	Level 5	Level 5	Level 5	Level 5	Cylindrical grip
6	Level 6	Level 6	Level 6	Level 6	Power grip

Table 4.3. Fuzzy rules.

The Four extracted features, i.e., MAV, IEMG, MAX, and RMS, were inputs to the FLC, and each input variable has six fuzzy sets, i.e., Level 1, Level 2, Level 3, Level 4, Level 5 and Level 6. The outputs of FLC were six hand gestures, which are Fine pinch, Tripod grip, Spherical grip, Fingers flexion, cylindrical grip, and power grip. Figure 4.4 shows the block diagram describing the FL classification process from a single sEMG channel for recognizing six different hand gestures.

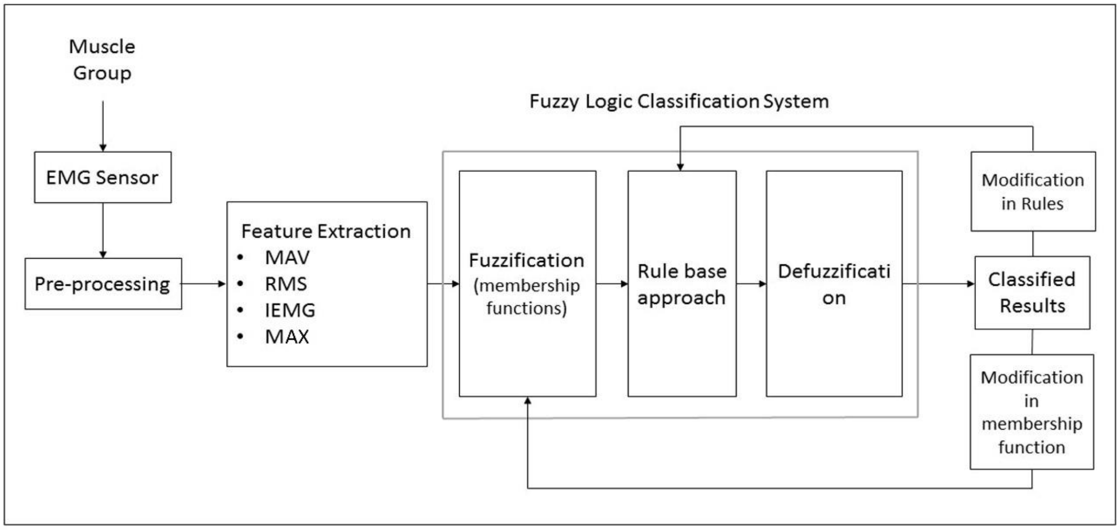

Figure 4.4 Block diagram for Fuzzy logic classification based control scheme.

4.2.5.2 Classifier's performance

For assessment of classification performance, the parameters such as accuracy, sensitivity, specificity, precision and F_1 score were determined. These statistical parameters are extensively used for analyzing the utility of classification-based systems (Gandolla et al. 2016). Accuracy (ACC) was defined as the ratio of the total number of correctly classified samples to the total number of samples. ACC was evaluated using equation (4.4), where

True positive (TP): gives the number of samples correctly classified for a specific hand gesture.

False positive (FP): provides the number of samples wrongly classified for the same hand gesture.

True negative (TN): furnishes the number of samples correctly classified as other hand gestures.

False negative (FN): gives the number of samples wrongly classified as the same hand gesture.

$$\text{Accuracy(ACC)} = \frac{(\sum \text{TP} + \sum \text{TN})}{(\sum \text{TP} + \sum \text{TN} + \sum \text{FP} + \sum \text{FN})} \quad (4.4)$$

The only accuracy is not adequate to decide the appropriate class since it does not include the misclassifications, and there can be systematic error bias (Castro, Arjunan, and Kumar 2015). Therefore the other parameters like sensitivity (SEN), specificity (SPE), precision (PR), and F_1 score were considered in this study and computed using equations (4.5)-(4.8).

Sensitivity was defined as the ratio of the total number of correctly classified samples for the specific gesture to that of the total number of classified samples for the same gesture.

$$\mathrm{Sensitivity(SEN)} = \frac{\sum \mathrm{TP}}{(\sum \mathrm{TP} + \sum \mathrm{FN})} \tag{4.5}$$

Specificity was defined as the ratio of the total number of correctly classified samples as the other gestures to that of the total number of classified samples as other gestures.

$$\mathrm{Specificity(SPE)} = \frac{\sum \mathrm{TN}}{(\sum \mathrm{TN} + \sum \mathrm{FP})} \tag{4.6}$$

Precision was defined as the ratio of the total number of correctly classified samples for the specific gesture to the total number of classified samples.

$$\mathrm{Precision(PR)} = \frac{\sum \mathrm{TP}}{(\sum \mathrm{TP} + \sum \mathrm{FP})} \tag{4.7}$$

$\mathrm{F_1}$ score was defined as the harmonic mean of precision and sensitivity. It analyzes the classifier's performance better than the accuracy.

$$\mathrm{F_1\ Score(F_1)} = \frac{2(\mathrm{SEN} * \mathrm{PR})}{(\mathrm{SEN} + \mathrm{PR})} \tag{4.8}$$

4.2.6 Real-time implementation and testing

4.2.6.1 Prosthetic hand development

Inmoov hand model parts were printed using Raised 3D N1 printer and were assembled as shown in Figure 4.5(a) (InMoov n.d.). The 3D printed hand was extrinsically actuated (i.e., the location of actuators outside the hand) using five high torque servomotors (MG-995) via tendons (Kargov et al. 2004). Each finger was individually activated through their servomotor. Pulleys attached to the motors were used to manipulate the tendons to provide flexion and extension of fingers. High tension fishing line of 0.60 mm diameter was utilized as tendons. The hand was capable of providing a total of 16 degrees of freedom (DOF). Silicon caps were installed at the tip of each finger to improve the gripping ability of the hand.

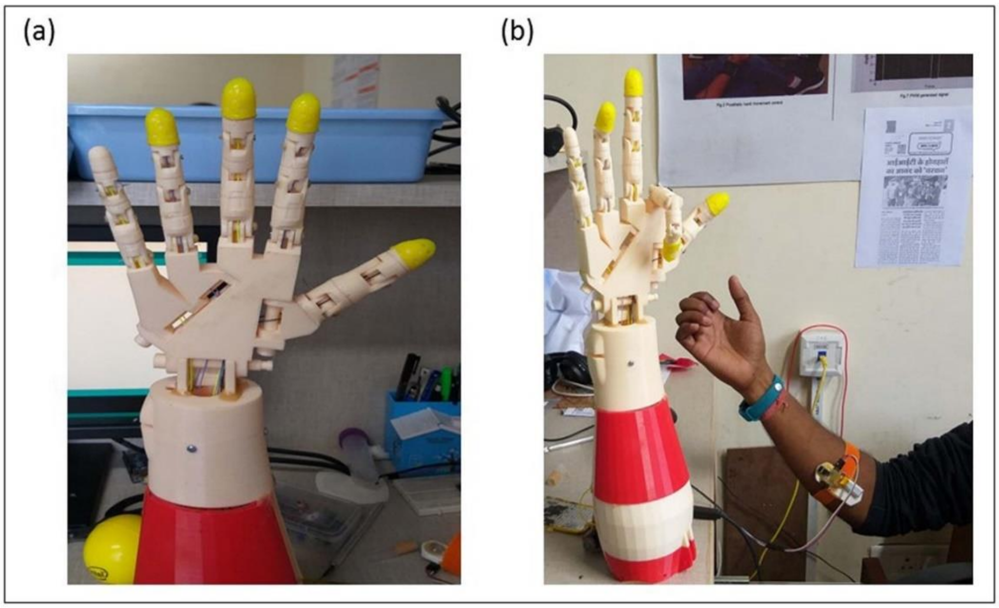

Figure 4.5 (a) Developed 3D printed hand prototype, (b) experimental setup for real-time operation of hand.

4.2.6.2 Control scheme

A control strategy in myoelectric prosthesis translates the classified features of the EMG signal to control command for actuation of the prosthetic device. The FL based classification scheme was further implemented in hardware for real-time operation of developed multi-DOF hand prototype. The classifier output (i.e., hand gestures in terms of weight) was fed to the threshold-based position controller to generate control signals to drive the servomotors linked mechanically with a 3D printed hand. The threshold control algorithm was employed to govern the servomotor position to get the desired flexion and extension of fingers. Figure 4.6 shows the scheme for controlling multifunctional prosthetic hands using a single-channel EMG signal from the forearm. All the software parts of the control scheme were performed on LabVIEW and were converted to Arduino programming code (using Arduino compatible compiler for LabVIEW). The Arduino microcontroller receives analog input from the EMG sensor and generates pulse width modulation (PWM) signal for the operation of servomotors. The microcontroller was integrated inside the hand assembly. All the electrical and electronic components present in the hand prototype receive power supply from a 5 V, 10000 mAh battery bank. The designed sEMG sensor was interfaced with the developed hand prototype to produce a multifunctional myoelectric hand prototype.

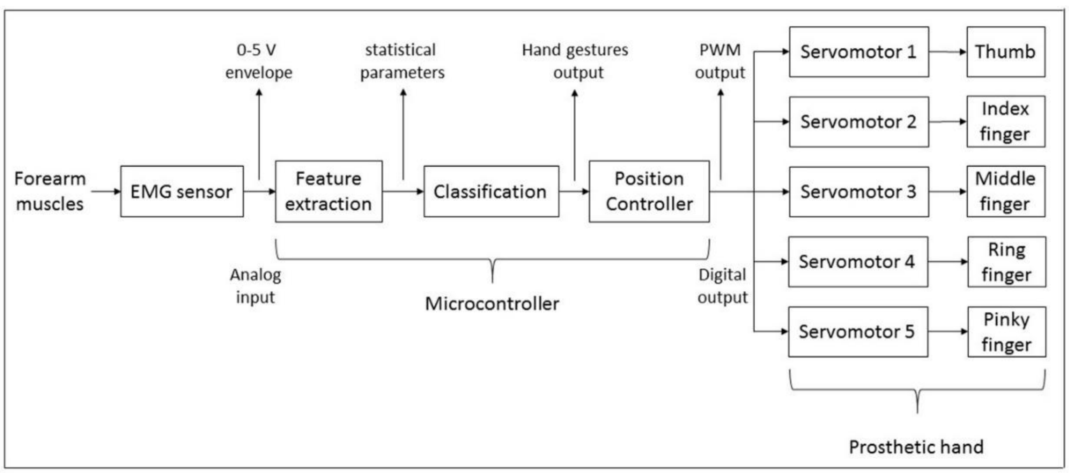

Figure 4.6 The control scheme for real-time control of the developed prosthetic hand.

4.2.6.3 Method for testing and analysis

The developed prosthetic hand setup was tested on five subjects (two amputees and three intact) for executing different grasping activities. Figure 4.5(b) describes the experimental setup for controlling prosthetic hand utilizing EMG signals from the user's forearm muscle. The EMG sensor was positioned at the flexor carpi ulnaris muscle of the participant's forearm through the velcro strap for providing an input signal to the prosthetic device. The participants were advised to keep their forearms at a stable position while testing. The hand prototype was fixed vertically upward on the table.

All five participants were asked to perform the six different grip actions of the hand using their six distinct levels of muscular contractions. Subjects attempted each grip action 20 times, and the number of correct attempts was noted. Each grip action was performed for about 30 s. Moreover, the time elapsed for performing each grip action was evaluated from the recorded video of hand operation, considering all the subjects. The elapsed times for accomplishing different grip patterns give the response times of the developed prosthetic hand.

4.3 Results

4.3.1 Sensor output

The EMG envelopes obtained for six distinct contraction levels of forearm muscles from a subject using the designed sensor are shown in Figure 4.7.

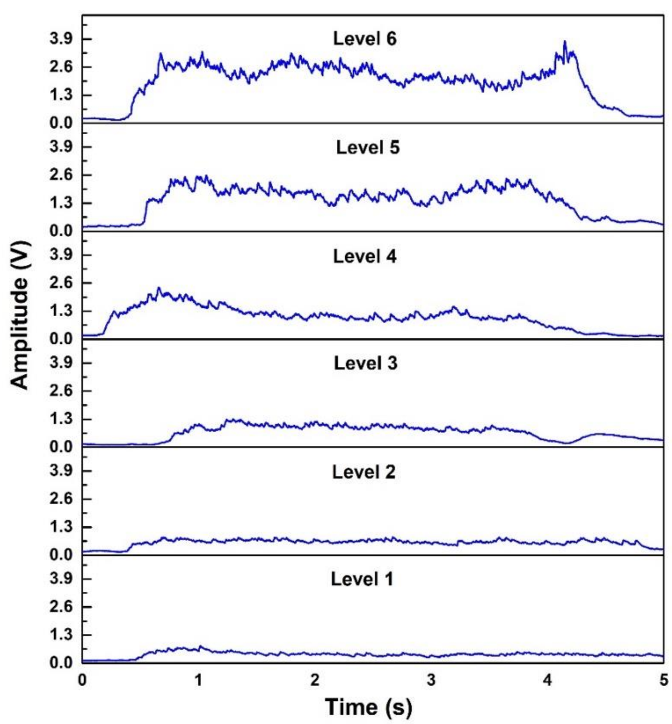

Figure 4.7 EMG envelopes for six levels of muscular contraction using the designed sensor.

4.3.2 Extracted features

The feature extraction process was performed by evaluating and analyzing four statistical features. Figure 4.8 describes the 3D plots showing the variation of four TD features, i.e., MAV, IEMG, MAX, and RMS, with six different levels of muscular contractions for all the subjects.

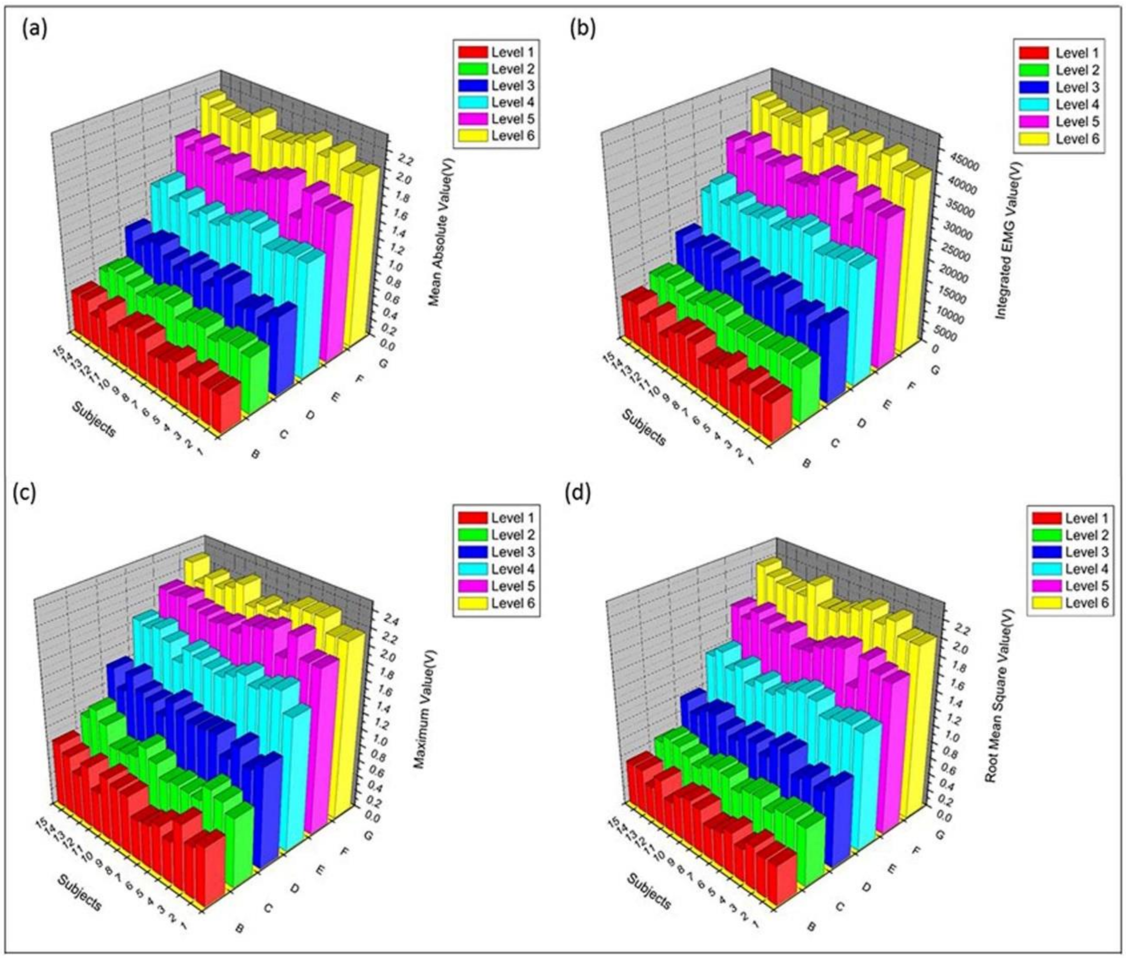

Figure 4.8 3D plot for variation of (a) MAV, (b) IEMG, (c) MAX, (d) RMS with different muscular contraction levels for all the subjects.

4.3.3 Classification performance

The performance of the FL system was tested for a total of 450 attempts (i.e., 75 attempts for each gesture). The percentage of success for classifying six hand gestures is described in Table 4.4.

Hand gesture	**Level number**	**Total number of testing attempts**	**Number of correctly classified motion**	**Number of wrongly classified motion**	**Percentage of success (%)**
Fine pinch	1	75	75	0	100
Tripod grip	2	75	69	6	92
Spherical grip	3	75	72	3	96
Fingers flexion	4	75	71	4	94.6
Cylindrical grip	5	75	70	5	93.3
Power grip	6	75	75	0	100
Overall success					95.98

Table 4.4. Achieved classification percentages for the six gestures.

In biomedical decision-making procedures, the ROC analysis technique is widely employed to determine the discrimination capability of the classification system (Taşar and Gülten 2017). In this work, FLC algorithm performance through ROC analysis for six hand activities is described in Table 4.5.

ROC analysis	**Hand Gestures**					
Classification output	**Fine pinch**	**Tripod grip**	**Spherical grip**	**Fingers flexion**	**Cylindrical grip**	**Power grip**
Fine pinch	75	0	0	0	0	0
Tripod grip	0	69	1	0	0	0
Spherical grip	0	6	72	4	0	0
Fingers flexion	0	0	2	71	5	0
Cylindrical grip	0	0	0	0	70	0
Power grip	0	0	0	0	0	75

Table 4.5. ROC analysis for each hand activity.

The five performance parameters determined using equation (4)-(8) are expressed in a 2 x 2 contingency table. Contingency matrices for each hand gesture are described in Table 4.6.

Fine pinch			**Tripod grip**			**Spherical grip**		
TP=75	FN=0	75	TP=69	FN=1	70	TP=72	FN=10	82
FP=0	TN=375	375	FP=6	TN=374	380	FP=3	TN=365	368
75	375	450	75	375	450	75	375	450
ACC=1.0			ACC=0.984			ACC=0.971		
SEN=1.0			SEN=0.985			SEN=0.878		
SPE=1.0			SPE=0.984			SPE=0.991		
PR=1.0			PR=0.92			PR=0.96		
F_1=1.0			F_1=0.951			F_1=0.917		
Fingers flexion			**Cylindrical grip**			**Power grip**		
TP=71	FN=7	78	TP=70	FN=0	75	TP=75	FN=0	75
FP=4	TN=368	372	FP=5	TN=375	375	FP=0	TN=375	375
75	375	450	75	375	450	75	375	450
ACC=0.975			ACC=0.988			ACC=1.0		
SEN=0.910			SEN=1.0			SEN=1.0		
SPE=0.989			SPE=0.986			SPE=1.0		
PR=0.946			PR=0.933			PR=1.0		
F1=0.927			F_1=0.965			F_1=1.0		

Table 4.6. Contingency matrices.

4.3.4 Real-time testing of the multi-functional prosthetic hand

The developed prosthetic hand implemented with FL classification based control strategy was tested in real-time to produce the six predefined grip patterns shown in Figure 4.9.

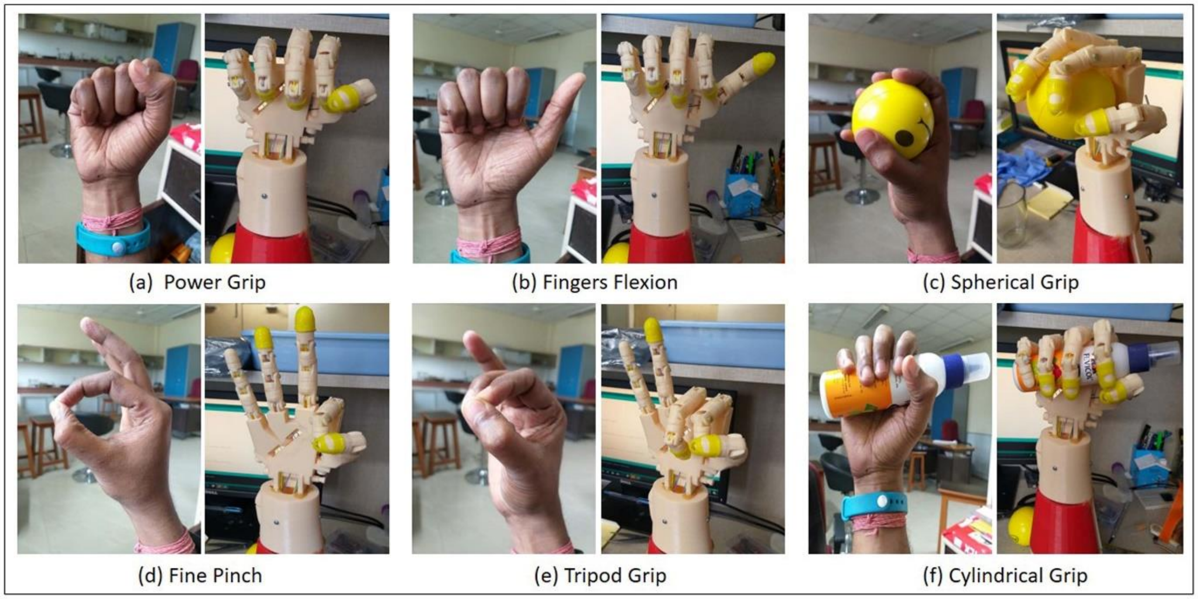

Figure 4.9 Six predefined grip patterns of the human hand and the grip patterns obtained by prosthetic hand.

With six grip patterns, the prosthetic hand was able to grasp objects of various shapes utilizing different levels of muscular contraction. Figure 4.10 shows the grasping actions performed by the prosthetic hand using the EMG signal of a subject.

Figure 4.10 Different grasping actions performed by the prosthetic hand utilizing EMG signal from a subject.

The number of correct grip actions performed by the subjects out of 20 attempts for each grip action is provided in Table 4.7. The last row of the table provides the average success % of all the subjects for accomplishing each grip pattern. The overall success rate for all the grip patterns was observed at 91.3 %.

Number of attempts (20)	**Numbers of correctly executed grip action**					
	Fine pinch	**Tripod grip**	**Spherical grip**	**Fingers flexion**	**Cylindrical grip**	**Power grip**
Subject 1	18	16	16	15	18	20
Subject 2	18	17	18	17	19	19
Subject 3	19	18	18	18	18	19
Subject 4	19	19	18	17	19	20
Subject 5	20	19	19	18	19	20
Average % of success	94	89	89	85	93	98

Table 4.7. The number of correct grip actions performed by the subjects.

Furthermore, the response times of the prosthetic hand evaluated for each grip pattern, considering all the subjects, are illustrated in the box whisker's plot shown in Figure 4.11. The plot shows the variation of response times of each grip action type for all the subjects in which average and standard deviation are indicated.

There were some movements observed for the forearm with respect to the elbow joint while doing real-time testing. But these movements did not affect the muscular contraction level in performing a specific grip activity. Each subject participated in the hand prosthesis trial for about two hours, and there was no report of muscle fatigue from any of them.

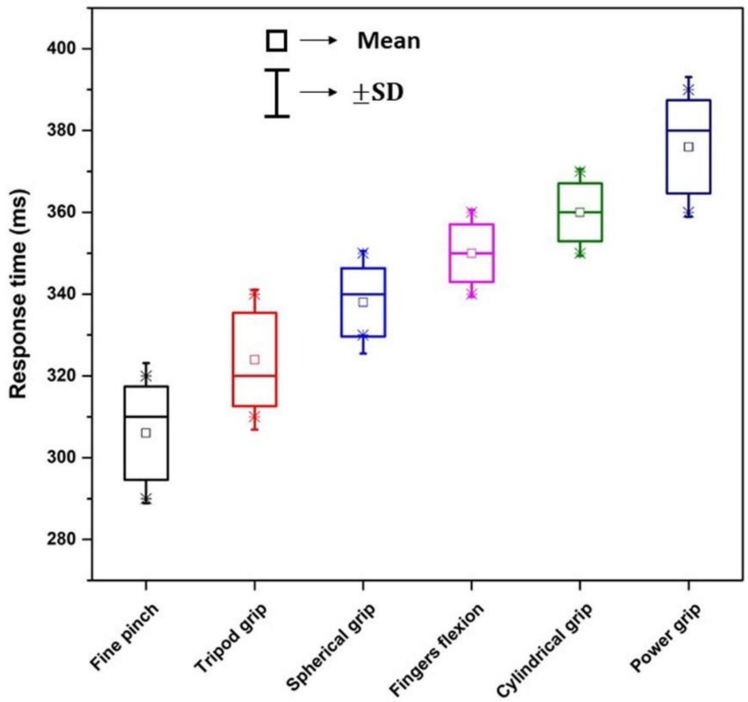

Figure 4.11 Variation of the response time of prosthetic hand for performing each grip pattern considering all the subjects.

4.4 Discussion

The designed EMG sensor was able to produce a linear and smooth envelope proportional to the level of muscular contraction. This attribute of the sensor allows the allocation of different contraction levels to identify various hand gestures.

The extracted features from the recorded EMG signals for all the subjects are distinguishable for every level, which is clear from the 3D plot shown in Figure 4.8. The time-domain features were used as a decent source of input for the Fuzzy logic classifiers to recognize the predefined hand gestures. Fuzzy systems can detect patterns in biomedical data that are not easily discoverable by other means. Fuzzy logic (FL) uses the tolerance of inaccuracy, ambiguity, and slight stretch, to attain controllable, robust, and affordable alternatives for classifications (Ajiboye and Weir 2005). Ahmad and Chappel classified the contraction on wrist muscles to control artificial hand using FL classifier and achieved an accuracy of 97 % (Ahmad, 2009).

Xie et al., 2014 suggested that the rule-based approaches within the FL schemes can mimic intentions more closely compared to the other classification systems (Xie et al. 2014).

In this study, all six hand gestures were identified, with an overall success rate of more than 94%. However, the determined performance parameters showed the average classification accuracy above 98% and the other parameters such as sensitivity, specificity, precision, and F1 score over 95%. Thus, the accuracy of the proposed system was observed comparable to that of multichannel channel EMG based classification performed by the researchers (Chan, Lam, and Parker 2000; Singh and Kumar 2008; Castro, Arjunan, and Kumar 2015; F. Wang, Oskoei, and Hu 2017). This approach reduces the overall cost and the complexity of the system and makes the approach more practical for the application of hand prosthesis control.

Moreover, utilizing EMG signal envelopes rather than EMG signal patterns for performing classification provides a more reliable approach requiring very little training effort and more intuitive for the user. Because pattern recognition based classification rely on matching of produced EMG patterns with the training patterns but these patterns tend to change significantly due to factors such as sweat, electrode shift, muscle fatigue, etc. (Hargrove, Englehart, and Hudgins 2008; Ortiz-Catalan et al. 2012; Roche et al. 2014; Stango, Negro, and Farina 2015).

Further, the FL classification scheme, along with the threshold control, was implemented in real-time to achieve six different grip patterns of the designed prosthetic hand, i.e., fine pinch, tripod grip, spherical grip, fingers flexion, cylindrical grip, and power grip. The subjects utilizing EMG signals for their distinct levels of muscular contractions could accomplish six different grasping activities with an overall success rate above 91%. The response time for executing different grip patterns was observed at less than 400 ms, which is an acceptable delay for myoelectric hand operations (Englehart, Hudgin, and Parker 2001). The prosthetic hand system with the designed control strategy was able to accomplish different grasping operations that can furnish activities of daily livings (ADLs).

4.5 Conclusion

As per this research, multiple operations, i.e., grip patterns, were obtained for the developed prosthetic hand using a single channel EMG sensor. The acquired data with the self-designed sensor were classified to identify six different hand gestures using the Fuzzy logic system. The classifier's overall performance was evaluated in terms of classification accuracy, sensitivity, precision, specificity, and F1 score for recognizing every gesture. The output gestures from the classifier were performed in real-time on the developed hand prototype. Using EMG signals for different synergies of forearm muscles, the hand was able to implement six distinct grip patterns for dexterous grasping of various-shaped objects with a very less number of training sessions. The developed hand validated on five subjects showed a success rate (>91%) and faster response for performing different grip actions. The developed multi-functional hand in the future can be validated for many users to see its tolerance level to external disturbances.

The one disadvantage of the proposed system is that its functional capability is confined to six hand actions. Also, there should be control over the grip force while grasping objects, which can be achieved by installing pressure sensors at the fingertips and implementing a closed-loop control system.

Moreover, such a multi-functional hand based on the single-channel EMG system can provide a low-cost solution to amputees for performing their primary tasks of daily living as compared to the commercially available hands.

4.6 References

Ahmad, S.A., 2009. Moving approximate entropy and its application to the electromyographic control of an artificial hand (Doctoral dissertation, University of Southampton).

Ahsan, M. R., M. I. Ibrahimy, and O. O. Khalifa. 2011. “Hand Motion Detection from EMG Signals by Using ANN Based Classifier for Human Computer Interaction.” In *Simulation and Applied Optimization 2011 Fourth International Conference on Modeling*, 1–6. https://doi.org/10.1109/ICMSAO.2011.5775536.

Ajiboye, A. B., and R. F. Weir. 2005. “A Heuristic Fuzzy Logic Approach to EMG Pattern Recognition for Multifunctional Prosthesis Control.” *IEEE Transactions on Neural Systems and Rehabilitation Engineering* 13 (3): 280–91. https://doi.org/10.1109/TNSRE.2005.847357.

Al-Mulla, Mohamed R., Francisco Sepulveda, and Martin Colley. 2011. “A Review of Non-Invasive Techniques to Detect and Predict Localised Muscle Fatigue.” *Sensors (Basel, Switzerland)* 11 (4): 3545–94. https://doi.org/10.3390/s110403545.

Al-Timemy, A. H., G. Bugmann, J. Escudero, and N. Outram. 2013. “Classification of Finger Movements for the Dexterous Hand Prosthesis Control With Surface Electromyography.” *IEEE Journal of Biomedical and Health Informatics* 17 (3): 608–18. https://doi.org/10.1109/JBHI.2013.2249590.

Arjunan, Sridhar, and Dinesh Kumar. 2010. “Decoding Subtle Forearm Flexions Using Fractal Features of Surface Electromyogram from Single and Multiple Sensors.” *Journal of NeuroEngineering and Rehabilitation* 7 (1): 53. https://doi.org/10.1186/1743-0003-7-53.

Arjunan, Sridhar Poosapadi. 2008 “Fractal Features of Surface Electromyogram: A New Measure for Low Level Muscle Activation,” 152.

“Bebionic Hand.” Accessed October 21, 2019. https://www.ottobockus.com/prosthetics/upper-limb-prosthetics/solution-overview/bebionic-hand/.

Belter, Joseph T., Jacob L. Segil, Aaron M. Dollar, and Richard F. Weir. 2013. “Mechanical Design and Performance Specifications of Anthropomorphic Prosthetic Hands: A Review.” *The Journal of Rehabilitation Research and Development* 50 (5): 599. https://doi.org/10.1682/JRRD.2011.10.0188.

Castro, Maria Claudia F., Sridhar P. Arjunan, and Dinesh K. Kumar. 2015. “Selection of Suitable Hand Gestures for Reliable Myoelectric Human Computer Interface.” *BioMedical Engineering OnLine* 14 (1): 30. https://doi.org/10.1186/s12938-015-0025-5.

Chan, F. H. Y., and F. K. Lam, and and P. A. Parker. 2000. “Fuzzy EMG Classification for Prosthesis Control.” *IEEE Transactions on Rehabilitation Engineering* 8 (3): 305–11. https://doi.org/10.1109/86.867872.

Cipriani, Christian, Marco Controzzi, and Maria Chiara Carrozza. 2011. “The SmartHand Transradial Prosthesis.” *Journal of NeuroEngineering and Rehabilitation* 8 (1): 29. https://doi.org/10.1186/1743-0003-8-29.

Cordella, Francesca, Anna Lisa Ciancio, Rinaldo Sacchetti, Angelo Davalli, Andrea Giovanni Cutti, Eugenio Guglielmelli, and Loredana Zollo. 2016. “Literature Review on Needs of Upper Limb Prosthesis Users.” *Frontiers in Neuroscience* 10 (May). https://doi.org/10.3389/fnins.2016.00209.

De Luca, Carlo J., Mikhail Kuznetsov, L. Donald Gilmore, and Serge H. Roy. 2012. "Inter-Electrode Spacing of Surface EMG Sensors: Reduction of Crosstalk Contamination during Voluntary Contractions." *Journal of Biomechanics* 45 (3): 555–61. https://doi.org/10.1016/j.jbiomech.2011.11.010.

Endo, T., H. Kawasaki, T. Mouri, Y. Ishigure, H. Shimomura, M. Matsumura, and K. Koketsu. 2011. "Five-Fingered Haptic Interface Robot: HIRO III." *IEEE Transactions on Haptics* 4 (1): 14–27. https://doi.org/10.1109/TOH.2010.62.

Englehart, K., B. Hudgin, and P. A. Parker. 2001. "A Wavelet-Based Continuous Classification Scheme for Multifunction Myoelectric Control." *IEEE Transactions on Biomedical Engineering* 48 (3): 302–11. https://doi.org/10.1109/10.914793.

Englehart, K, B Hudgins, P. A Parker, and M Stevenson. 1999. "Classification of the Myoelectric Signal Using Time-Frequency Based Representations." *Medical Engineering & Physics* 21 (6): 431–38. https://doi.org/10.1016/S1350-4533(99)00066-1.

Erim , Z., and W. Lin. 2008. "Decomposition of Intramuscular EMG Signals Using a Heuristic Fuzzy Expert System." *IEEE Transactions on Biomedical Engineering* 55 (9): 2180–89. https://doi.org/10.1109/TBME.2008.923915.

Esposito, Daniele, Emilio Andreozzi, Antonio Fratini, Gaetano D Gargiulo, Sergio Savino, Vincenzo Niola, and Paolo Bifulco. 2018. "A Piezoresistive Sensor to Measure Muscle Contraction and Mechanomyography." *Sensors (Basel, Switzerland)* 18 (8). https://doi.org/10.3390/s18082553.

Gandolla, Marta, Simona Ferrante, Giancarlo Ferrigno, Davide Baldassini, Franco Molteni, Eleonora Guanziroli, Michele Cotti Cottini, Carlo Seneci, and Alessandra Pedrocchi. 2016. "Artificial Neural Network EMG Classifier for Functional Hand Grasp Movements Prediction:" *Journal of International Medical Research*, September. https://doi.org/10.1177/0300060516656689.

Geng, Weidong, Yu Du, Wenguang Jin, Wentao Wei, Yu Hu, and Jiajun Li. 2016. "Gesture Recognition by Instantaneous Surface EMG Images." *Scientific Reports* 6: 36571. https://doi.org/10.1038/srep36571.

Gini, Giuseppina, Matteo Arvetti, Ian Somlai, and Michele Folgheraiter. 2012. "Acquisition and Analysis of EMG Signals to Recognize Multiple Hand Movements for Prosthetic Applications." *Applied Bionics and Biomechanics* 9 (2): 145–55. https://doi.org/10.1155/2012/792359.

"Hand and Forarm – InMoov.". Accessed April 28, 2019. http://inmoov.fr/hand-and-forarm/.

Hargrove, Levi, Kevin Englehart, and Bernard Hudgins. 2008. "A Training Strategy to Reduce Classification Degradation Due to Electrode Displacements in Pattern Recognition Based Myoelectric Control." *Biomedical Signal Processing and Control*, Surface Electromyography, 3 (2): 175–80. https://doi.org/10.1016/j.bspc.2007.11.005.

"I-Limb Quantum | Touch Bionics." Accessed April 12, 2019. http://touchbionics.com/products/active-prostheses/i-limb-quantum.

Kargov, Artem, Christian Pylatiuk, Jan Martin, Stefan Schulz, and Leonhard Döderlein. 2004. "A Comparison of the Grip Force Distribution in Natural Hands and in Prosthetic Hands." *Disability and Rehabilitation* 26 (12): 705–11. https://doi.org/10.1080/09638280410001704278.

Khushaba, R. N., A. H. Al-Timemy, A. Al-Ani, and A. Al-Jumaily. 2017. "A Framework of Temporal-Spatial Descriptors-Based Feature Extraction for Improved Myoelectric

Pattern Recognition." *IEEE Transactions on Neural Systems and Rehabilitation Engineering* 25 (10): 1821–31. https://doi.org/10.1109/TNSRE.2017.2687520.

Lobo-Prat, Joan, Peter N. Kooren, Arno HA Stienen, Just L. Herder, Bart FJM Koopman, and Peter H. Veltink. 2014. "Non-Invasive Control Interfaces Forintention Detection in Active Movement-Assistive Devices." *Journal of NeuroEngineering and Rehabilitation* 11 (1): 168. https://doi.org/10.1186/1743-0003-11-168.

"Michelangelo Prosthetic Hand." Accessed April 12, 2019. https://www.ottobockus.com/prosthetics/upper-limb-prosthetics/solution-overview/michelangelo-prosthetic-hand/.

Nazmi, Nurhazimah, Mohd Azizi Abdul Rahman, Shin-Ichiroh Yamamoto, Siti Anom Ahmad, Hairi Zamzuri, and Saiful Amri Mazlan. 2016. "A Review of Classification Techniques of EMG Signals during Isotonic and Isometric Contractions." *Sensors* 16 (8): 1304. https://doi.org/10.3390/s16081304.

Ortiz-Catalan, Max, Rickard Brånemark, Bo Håkansson, and Jean Delbeke. 2012. "On the Viability of Implantable Electrodes for the Natural Control of Artificial Limbs: Review and Discussion." *BioMedical Engineering OnLine* 11 (1): 33. https://doi.org/10.1186/1475-925X-11-33.

Oskoei, M. A., and H. Hu. 2008. "Support Vector Machine-Based Classification Scheme for Myoelectric Control Applied to Upper Limb." *IEEE Transactions on Biomedical Engineering* 55 (8): 1956–65. https://doi.org/10.1109/TBME.2008.919734.

Phinyomark, Angkoon, Pornchai Phukpattaranont, and Chusak Limsakul. 2012. "Fractal Analysis Features for Weak and Single-Channel Upper-Limb EMG Signals." *Expert Systems with Applications* 39 (12): 11156–63. https://doi.org/10.1016/j.eswa.2012.03.039.

Prakash, Alok, Shiru Sharma, and Neeraj Sharma. 2019. "A Compact-Sized Surface EMG Sensor for Myoelectric Hand Prosthesis." *Biomedical Engineering Letters* 9 (4): 467–79. https://doi.org/10.1007/s13534-019-00130-y.

Roche, Aidan D., Hubertus Rehbaum, Dario Farina, and Oskar C. Aszmann. 2014. "Prosthetic Myoelectric Control Strategies: A Clinical Perspective." *Current Surgery Reports* 2 (3): 44. https://doi.org/10.1007/s40137-013-0044-8.

"Signal-Dependent Wavelets for Electromyogram Classification." 2005. *Biological Engineering* 43: 6.

Singh, V. P., and D. K. Kumar. 2008. "Classification of Low-Level Finger Contraction from Single Channel Surface EMG." In *2008 30th Annual International Conference of the IEEE Engineering in Medicine and Biology Society*, 2900–2903. https://doi.org/10.1109/IEMBS.2008.4649809.

Stango, Antonietta, Francesco Negro, and Dario Farina. 2015. "Spatial Correlation of High Density EMG Signals Provides Features Robust to Electrode Number and Shift in Pattern Recognition for Myocontrol." *IEEE Transactions on Neural Systems and Rehabilitation Engineering* 23 (2): 189–98. https://doi.org/10.1109/TNSRE.2014.2366752.

Supuk, Tamara Grujic, Ana Kuzmanic Skelin, and Maja Cic. 2014. "Design, Development and Testing of a Low-Cost SEMG System and Its Use in Recording Muscle Activity in Human Gait." *Sensors (Basel, Switzerland)* 14 (5): 8235–58. https://doi.org/10.3390/s140508235.

Taşar, Beyda, and Arif Gülten. 2017. "EMG-Controlled Prosthetic Hand with Fuzzy Logic Classification Algorithm." *Modern Fuzzy Control Systems and Its Applications*, August. https://doi.org/10.5772/intechopen.68242.

Tavakoli, Mahmoud, Carlo Benussi, and Joao Luis Lourenco. 2017. "Single Channel Surface EMG Control of Advanced Prosthetic Hands." *Expert Syst. Appl.* 79 (C): 322–332. https://doi.org/10.1016/j.eswa.2017.03.012.

"VINCENTevolution 3." Accessed April 12, 2019. https://vincentsystems.de/en/prosthetics/vincent-evolution-3/.

Wang, Fang, Mohammadreza Asghari Oskoei, and osheng Hu. 2017. "Multi-Finger Myoelectric Signals for Controlling a Virtual Robotic Prosthetic Hand." *International Journal of Modelling, Identification and Control* 27 (3): 181. https://doi.org/10.1504/IJMIC.2017.083780.

Wang, Jingpeng, Liqiong Tang, and John E Bronlund. 2013. "Surface EMG Signal Amplification and Filtering." *International Journal of Computer Applications* 82 (1): 15–22. https://doi.org/10.5120/14079-2073.

Wang, Nianfeng, Kunyi Lao, and Xianmin Zhang. 2017. "Design and Myoelectric Control of an Anthropomorphic Prosthetic Hand." *Journal of Bionic Engineering* 14 (1): 47–59. https://doi.org/10.1016/S1672-6529(16)60377-3.

Wu, Yansheng, Shili Liang, Ling Zhang, Zongqian Chai, Chunlei Cao, and Shuangwei Wang. 2018. "Gesture Recognition Method Based on a Single-Channel SEMG Envelope Signal." *EURASIP Journal on Wireless Communications and Networking* 2018 (1). https://doi.org/10.1186/s13638-018-1046-0.

Xie, Hong-Bo, Tianruo Guo, Siwei Bai, and Socrates Dokos. 2014. "Hybrid Soft Computing Systems for Electromyographic Signals Analysis: A Review." *BioMedical Engineering OnLine* 13 (1): 8. https://doi.org/10.1186/1475-925X-13-8.